Behaviour of biomass multicomponent ashes as adsorbents

Sunil K. Deokar[1], Sachin A. Mandavgane[1,*] and Bhaskar D. Kulkarni[2]

[1]Department of Chemical Engineering, VNIT, Nagpur 440 010, India
[2]CSIR-National Chemical Laboratory, Pune 411 008, India

Physico-chemical characteristics of rice husk ash and baggase fly ash, commonly referred to as biomass ashes (BMA), enable their use as adsorbents. Contrary to normal expectations, it is observed that larger particles have more number, narrower and deeper pores than smaller particles. As a consequence they have higher pore volume, total surface area and hence adsorption capacity. Also, the uptake rate of adsorption depends on the silica to carbon ratio, which is seen to be smaller for larger particles and hence they take a longer time to reach equilibrium. The extent of carbon content determines the capacity, whereas silica to carbon ratio determines the kinetics of adsorption. Removal of 2,4-dichlorophenoxy acetic acid, from aqueous solution was chosen as a representative case for study and the results obtained are compared with earlier reported results.

Keywords: Adsorption capacity, bagasse, biomass ash, rice husk, silica to carbon ratio.

BIOMASS materials, viz. bagasse, rice husk, rice straw, etc. (~500 million metric tonnes per year) have been used for power generation owing to their potential as an energy source[1]. Each tonne of rice husk and bagasse after combustion produces 25% rice husk ash (RHA) and 2.4% bagasse fly ash (BFA) respectively[2,3]. Assuming complete milling of 157 million tonnes (mt) of rice and crushing of 342 mt of sugarcane produced in 2011 (ref. 4), the generation of rice husk (22% of rice production) and bagasse (26% of sugarcane production) would be approximately 35 and 89 mt respectively, which on fueling the boiler produces 9 mt RHA and 2 mt BFA. Besides combustion, a detailed physico-chemical characterization of biomass ashes (BMA, i.e. RHA and BFA) suggests two additional applications, viz. as an adsorbent for removal of pollutants and as a binding agent in construction[5–8].

Batch adsorption study evaluates the effects of adsorbate concentration, adsorbent dosages, contact time, solution pH, temperature and particle size of the adsorbents. Most studies generally conclude that smaller particle size of the adsorbent due to larger surface area favours adsorption[9–13]. In the present study, detailed physico-chemical characteristics of different particle size fractions of BMA have been investigated. Surface properties like BET surface area, pore diameter, pore volume and chemical composition particularly silica to carbon ratio have also been investigated. To study the effect of these parameters on adsorption, removal of 2,4-dichlorophenoxy acetic acid (2,4-D) from aqueous solution using BMA has been chosen as a representative case.

*For correspondence. (e-mail: sam@che.vnit.ac.in)

Materials and methods

Adsorbent

RHA and BFA were obtained from M/S Yash Agro Ltd, Nagpur, India and M/S Wainganga Sugar and Power Ltd, Bhandara (India) respectively. Rice husk and bagasse were used as solid fuel to fire boiler in these industries. Proximate analysis of BMA was carried out using standard method. Particle size distribution was determined using BSS standard sieves. The surface area, pore diameter and pore volume were determined by the Brunaer–Emmett–Teller (BET) method using Micromeritics, ASAP 2010 instrument. The elemental chemical contents of BMA were determined by performing XRF analysis (PAN Analytical Model no. PW 2403). CHNS analysis was done using Elemental Analyser (Elementar Germany model: Vario Macro Cube). Presence of functional groups on the surface was investigated by FTIR analysis performed on Shimadzu IR-Affinity-1 model. The morphology of BMA was examined using scanning electron microscope (SEM, JSM 7600F). Before morphology study, BMA was coated with thin platinum layer using Auto Fine Coater (JFC-1600).

Adsorbate

Analytical grade 2,4-D (99.9% pure; Sigma Aldrich) was used without any treatment. Table 1 shows the molecular formula and properties of 2,4-D.

Table 1. Properties of 2,4-D

Molecular formula	$C_8H_6Cl_2O_3$
Molecular weight	221.00 g/mol
Solubility in water	890 mg/l
Molecular size (x, y, z; nm)	1.29 × 0.73 × 0.42

Batch adsorption study

Stock solution of 400 mg/l was prepared by dissolving accurately weighed quantity of 2,4-D in double-distilled water. Batch adsorption was studied by adding predefined quantity of BMA in 2,4-D solution taken in 50 ml glass vials. The vials were agitated in constant-temperature water bath. Equilibrium concentration of supernatant after centrifugation was determined on UV/VIS spectrophotometer (UV 1800, Shimadzu, Japan) at 283 nm. Experiments were performed in triplicate under identical conditions and average values have been reported. The per cent removal, adsorption capacity Q_t (mg/g) at any time t, and adsorption capacity Q_e (mg/g) at equilibrium were calculated as follows

$$\% \text{ Removal} = \left(\frac{C_0 - C_e}{C_0} \right) \times 100, \quad (1)$$

$$Q_t = \frac{(C_0 - C_t)V}{W}, \quad (2)$$

$$Q_e = \frac{(C_0 - C_e)V}{W}, \quad (3)$$

where C_0 (mg/l) and C_e (mg/l) are the initial and equilibrium concentration of 2,4-D respectively, V (l) is the volume of the solution, and W (g) is adsorbent mass. Effect of contact time and particle size of BMA on 2,4-D removal was also studied.

Results and discussion

Characterization of BMA

Particle size distribution of BMA (Table 2) was determined according to ASTM D422. It appears that the adsorbents have non uniform distribution of particles with the average particle size of RHA and BFA to be 144 and 118 μm respectively. Also the adsorbents contain more ash and volatile organic matter as can be seen from the physico-chemical characteristics of BMA (Table 3). BFA contains more fixed carbon than RHA and is confirmed by CHNS analysis and for the same size fractions show higher surface area and porosity. Although the chemical composition of RHA and BFA is qualitatively similar, they differ quantitatively. This significantly influences adsorbent properties. The nature of silica, crystalline or amorphous, depends upon combustion temperature. The literature reports the presence of cristobalite and quartz form of silica in RHA, and only quartz form in BFA[14]. Metal oxides play a vital role in the adsorption process as they form positive charges on the adsorbent surface when put in water. BJH adsorption–desorption analysis helps in understanding the proportion of pore area and pore volume occupied by micro-, meso- and macropores. In RHA, the micropores and mesopores occupy 5.31% and 93.91% of total (BJH adsorption) pore area respectively. Similarly, for BFA these values are 9.57% and 90.27% respectively. The micropore and mesopore volumes are 1.30%; 4.17% and 88.66%; 91.88% of total (BJH adsorption) pore volume for RHA and BFA respectively. So it can be deduced that BMA is predominantly mesoporous, which is highly desirable for a good adsorbent.

The scanning electron photomicrographs in Figure 1 *a* and *b* reveal the particle size and porosity, and suggest

Table 2. Particle size distribution of BMA

Particle size (mm)	RHA (wt %)	Particle size (mm)	RHA (wt %)
0.500–0.354	10.00	≥1.240	1.50
0.354–0.300	1.50	1.200–1.000	0.50
0.300–0.251	6.00	1.000–0.853	2.00
0.251–0.178	12.50	0.853–0.354	4.00
0.178–0.152	15.50	0.354–0.251	12.00
0.152–0.125	10.50	0.251–0.178	15.00
0.125–0.104	8.00	0.178–0.104	26.00
0.104–0.089	5.50	≤0.104	39.00
≤0.089	30.50		

Table 3. Physico-chemical characterization of BMA

	Characteristics	RHA	BFA
Proximate analysis	Moisture %	1.80	6.30
	Ash %	89.87	40.14
	Volatile matter %	6.19	42.46
	Fixed carbon %	2.14	11.10
Chemical analysis	SiO_2 %	81.78	36.14
	Al_2O_3 %	4.08	1.10
	K_2O %	1.87	2.32
	Fe_2O_3 %	1.27	1.62
	CaO %	1.27	3.10
	Rest others	3.06	5.73
CHN analysis	C %	5.85	47.37
	H %	0.48	2.04
	N %	0.82	1.59
	S %	0.27	0.43
	O % (balance)	92.58	48.57
Surface area (m^2/g)	Single point	33	51
	BET	33	51
	BJH adsorption cumulative	26	21
	BJH desorption cumulative	36	24
Pore volume (cm^3/g)	Single-point total	[a]2.69×10^{-3}	[b]4.96×10^{-2}
	BJH adsorption cumulative	5.30×10^{-2}	7.14×10^{-2}
	BJH desorption cumulative	5.25×10^{-2}	6.56×10^{-2}
Pore diameter (Å)	BJH adsorption average	80.60	132.42
	BJH desorption average	56.93	109.12

[a]Pore less than 20 Å; [b]pore less than 867 Å.

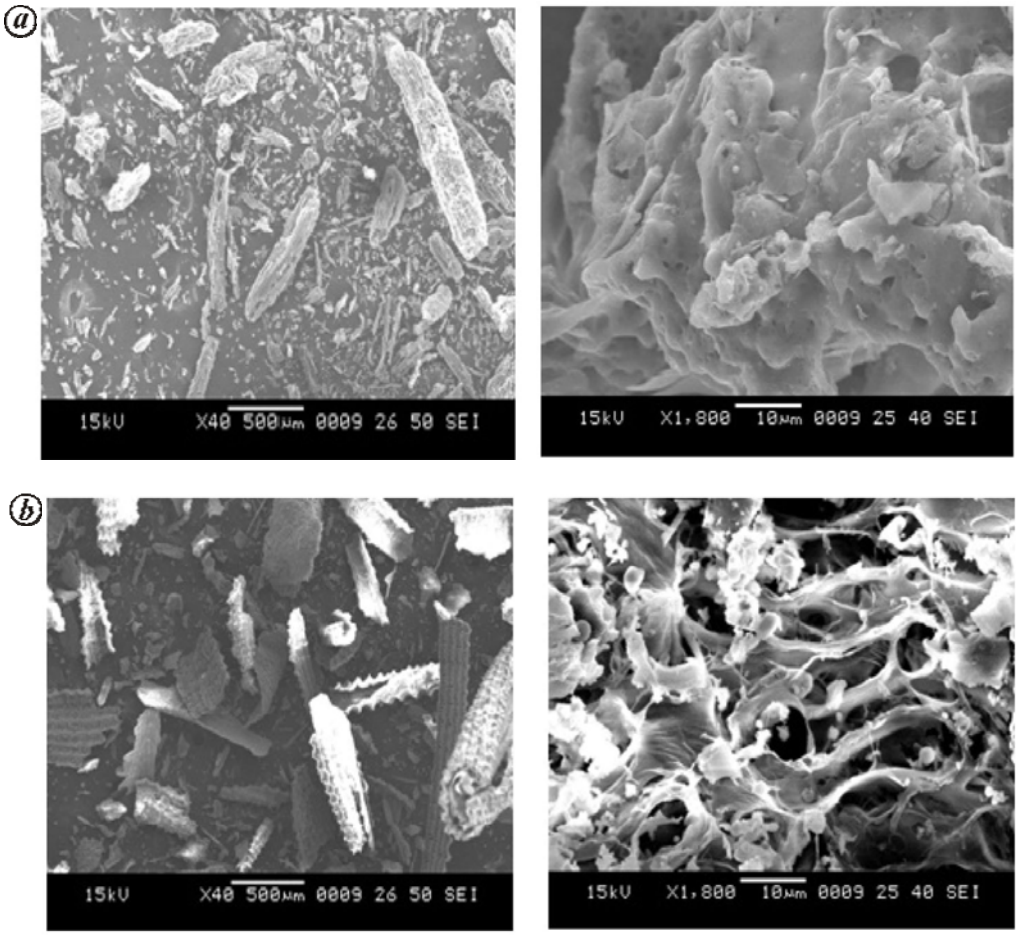

Figure 1. Scanning electron photomicrograph of (***a***) RHA and (***b***) BFA.

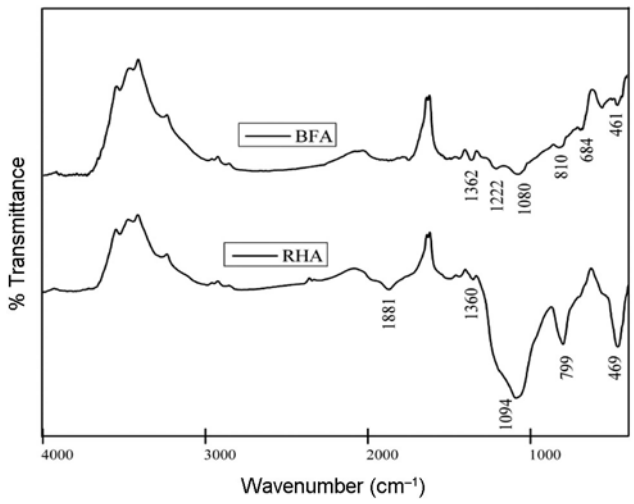

Figure 2. FTIR spectra of RHA and BFA.

different nature of each BMA. Comparison at lower magnification indicates the presence of more number of larger particles in BFA (Figure 1 *b*) than RHA (Figure 1 *a*), whereas the aspect ratio of BFA and RHA is in the range 2.6 : 1 to 4.4 : 1 and 2.4 : 1 to 4.8 : 1 respectively. Higher magnification clearly shows more pores in BFA than RHA. The circular and elongated pores can be easily observed in BFA; some pores seem internally connected. RHA has a slightly platelet-like structure with smaller pores.

FTIR spectra of RHA and BFA indicate similar functional groups in them. For both spectra (Figure 2), the 1667–2000 cm^{-1} band indicates the weak combinations and overtone absorption. The peaks in this region are assigned to mono to hexasubstitution of aromatic ring[15]. The bands in the region 1360–1380 cm^{-1} are attributed to the aromatic C–H and carboxyl–carbonate structures[16]. The peaks at 1080 cm^{-1} in BFA and 1094 cm^{-1} in RHA are the asymmetric stretching of Si–O–Si. The stretching vibration of Si–O at 684 cm^{-1} is characteristic of quartz in BFA, whereas stretching vibration at 799 cm^{-1} in RHA corresponds to H–C bond. In BFA, the weak peak at 461 cm^{-1} is an indication of bending mode of internal tetrahedral (O–Si–O)[17,18]. In RHA, the peak at 469 cm^{-1} is due to the presence of Si–H bond[19]. In the BFA spectrum, the peaks at 1222 and 810 cm^{-1} are indicative of amorphous silica[20].

Effect of adsorbent dosage

The adsorbent dosages of RHA and BFA were found to increase from 0.5 to 7 g/30 ml and 0.25 to 1.5 g/25 ml of 100 mg/l 2,4-D solution respectively. The experiments were performed for 12 h at pH 3.5. The maximum removal for RHA (4 g) and BFA (1 g) was found to be 83% and 90% respectively. Significant increase in 2,4-D removal was not observed for higher loading of BMA and hence for further studies, 4 g RHA and 1 g BFA were selected as the optimum adsorbent loading per 30 and 25 ml of adsorbate solution respectively.

Effect of contact time and initial concentration

The effect of contact time was studied using 2,4-D solutions of 100 and 200 mg/l concentration. The inside plot for RHA (Figure 3) demonstrates the same nature of curves for each solution. For both solutions, the equilibrium time for RHA was found to be 15 min, whereas for BFA it was 3 and 5 h respectively. The removal of 2,4-D increases with initial concentration of solution. This is due to higher mass transfer driving force at higher concentrations. The literature has reported similar results on banana stalk activated carbon[21].

Relation between particle size and surface area

Table 4 shows the particle size, pore diameter and pore volume of the samples. It is observed that larger particles have deeper pores of smaller opening, while smaller particles have shallow pore of wider opening. Smaller particles have bowl-type pores, while larger particles have cylindrical pores. Pore shape and dimensions of the two adsorbents affect the kinetics and capacity of adsorption. The literature has reported the role of pore properties on adsorption kinetics[13]. This is further discussed in the following sections. As determined here the larger particles, multi-component in nature, have smaller pores, whereas smaller particles have larger pores. As the particle size decreases the pore walls contact each other and collapse to form a bigger pore. This apparently creates a situation of smaller particles of larger pore and therefore lesser internal surface area. A probable reason for lesser BET surface area for smaller particles may be the blocking of pores (mesopores/macropores) by submicrometre-scale particles. Secondly, there may be non-porous fines present in BMA, which predominantly ended up in smaller particle size fractions[13].

The literature reports the use of different materials for adsorption of 2,4-D. Activated carbon, prepared from date stone[22] and corncob[23] having BET surface area 763.40 and 1273.91 m^2/g and average pore diameter as 26.184 and 30.26 Å respectively, were used. Tang *et al.*[24] used iron oxide, nanoparticles-doped carboxylic, ordered mesoporous carbon having 1054.50 m^2/g surface area and 1.85 cm^3/g pore volume. Zhang *et al.*[25] used magnetite–graphene oxide-layered double hydroxide composites (MGL) of surface area 71.9 m^2/g and pore volume 0.440 cm^3/g.

Effect of particle size and composition on adsorption capacity

Adsorption being a surface phenomenon is generally favoured by reduction in particle size. It is reported that smaller biomass particles have higher adsorption capacity than larger particles[9]. Higher adsorbate uptake is found even for (steel and fertilizer) industry waste[11], smaller bottom ash particles[12] and spent bleaching earth on

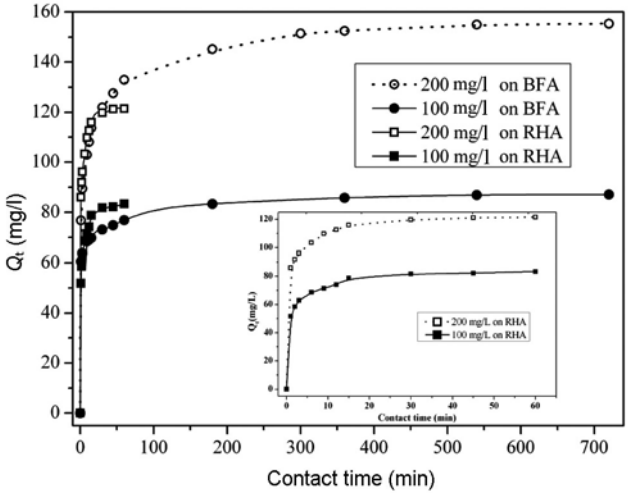

Figure 3. Effect of contact time and initial concentration on removal of 2,4-D.

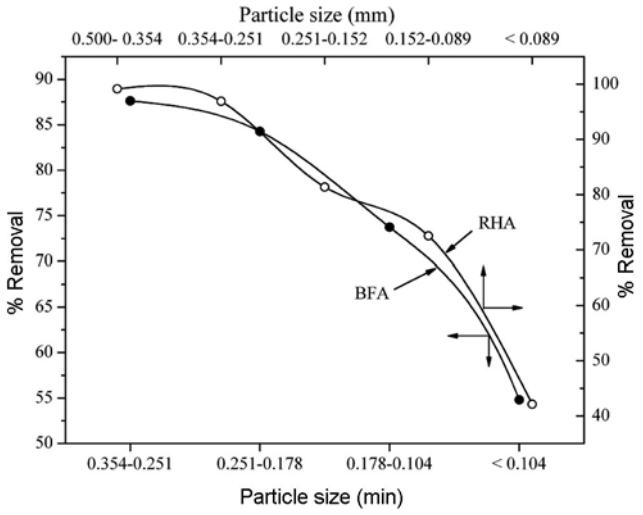

Figure 4. Effect of particle size of BMA on % removal where C_0 = 100 mg/l.

Table 4. Characteristics of different size fractions of BMA

Particle size (mm)	BET surface area (m^2/g)	Pore diameter (nm)	Pore volume (cm^3/g)	Carbon (%) from C, H, N analysis	SiO_2 (%) from XRF analysis	SiO_2/C ratio
RHA						
0.500–0.354	92	9.37	1.44×10^{-1}	12.72	76.59	6.02
0.354–0.251	44	10.35	9.28×10^{-2}	5.29	78.10	14.76
0.251–0.152	26	12.00	6.13×10^{-2}	3.38	79.80	23.60
0.152–0.089	17	13.81	4.57×10^{-2}	2.92	83.46	28.58
<0.089	13	16.15	3.78×10^{-2}	2.72	86.59	31.83
BFA						
0.354–0.251	98	7.09	7.05×10^{-2}	57.33	6.93	0.12
0.251–0.178	84	9.08	5.71×10^{-2}	42.82	9.77	0.29
0.178–0.104	62	10.15	5.14×10^{-2}	33.66	29.00	0.86
<0.104	35	11.76	4.41×10^{-2}	24.29	49.13	2.02

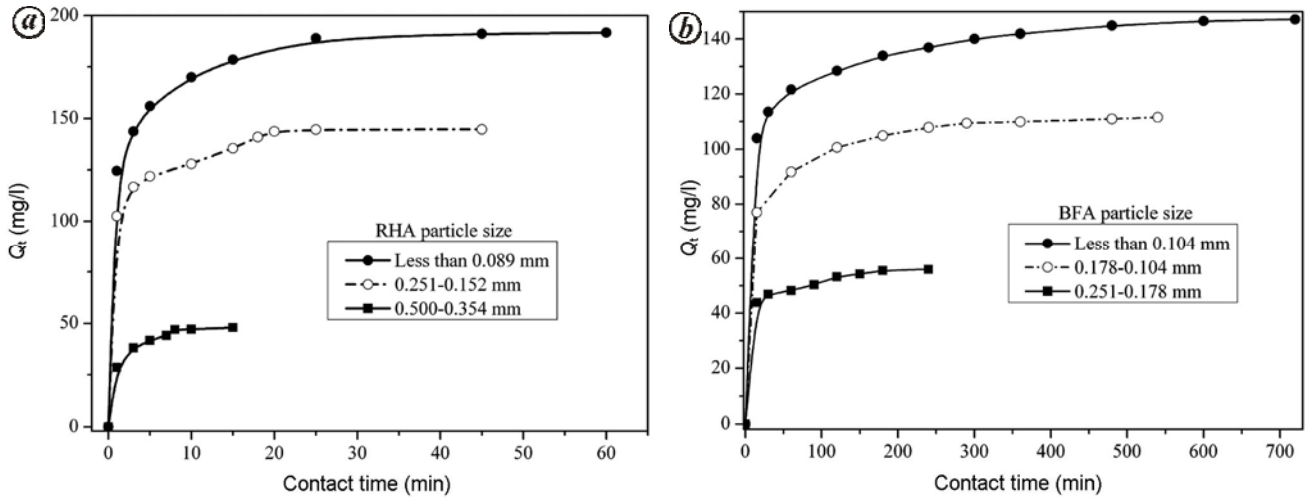

Figure 5. Effect of particle size of (***a***) RHA and (***b***) BFA on equilibrium time ($C_0 = 200$ mg/l, $W = 4$ g/30 ml) for (***a***) and $C_0 = 200$ mg/l, $W = 1$ g/25 ml for (***b***).

account of higher surface area[26]. We used different size fractions of BMA particles (Table 4) to study the effect of surface characteristics on adsorption. Adsorption capacity is directly proportional to BET surface area and hence larger particles of BMA with more BET surface area should give higher removal. This is experimentally validated and presented in Figure 4. Thus these adsorbents have demonstrated findings related to particle size, BET surface area and hence adsorption capacity.

It is observed (Table 4) that SiO_2/C (silica to carbon) ratio varies inversely with particle size of BMA. This ratio is one of the important parameters to explain the behaviour of BMA as a potential adsorbent. pHzpc of silica is 2.2 (ref. 27), whereas that of BMA is 8–9 (refs 19, 28). Hence when BMA is immersed in water (pH ~ 7), the silica in it offers negative charge. It can be deduced that the removal of 2,4-D would be primarily due to carbon, as 2,4-D being anionic in aqueous solution gets repelled by silica.

The surface is relatively more negative when the proportion of silica in BMA is higher. Thus BMA with lesser silica is a better adsorbent for anionic species like 2,4-D. Carbon fraction in BMA determines the capacity of adsorption, whereas silica fraction decides the kinetics. Hence higher adsorption capacity can be achieved by smaller SiO_2/C ratio and larger particle size fraction. The evidence for this is provided in Figure 4.

Effect of particle size and composition on equilibrium time

To study the effect of particle size and composition on equilibrium time, experiments were performed using 200 mg/l 2,4-D solution. Results are shown in Figure 5 *a* (for RHA) and *b* (for BFA). Both the adsorbents show higher equilibrium time and equilibrium capacity for larger particle size. As discussed earlier, larger particles have deeper pores; thereby the adsorbate molecule has to

Table 5. Kinetic rate constants for different particle size fractions of BMA

		Pseudo first-order		Pseudo second-order			
Adsorbent (mm)	Q_e expt (mg/g)	k_1 (min^{-1})	Q_e (mg/g)	k_2 (g mg^{-1} min^{-1})	Q_e (mg/g)	R^2	$t_{1/2}$ (min)
RHA	0.87	0.15	0.29	1.73	0.90	0.998	0.642
<0.089	0.35	0.57	0.38	2.77	0.38	0.995	0.950
0.251–0.152	1.08	0.17	0.43	1.05	1.10	0.997	0.865
0.500–0.354	1.44	0.11	0.49	0.61	1.47	0.999	1.115
BFA	3.81	1.20×10^{-2}	1.35	4.91×10^{-2}	3.82	0.999	5.331
<0.104	1.40	1.80×10^{-2}	0.50	8.77×10^{-2}	1.43	0.997	7.973
0.178–0.104	2.75	1.30×10^{-2}	1.15	3.07×10^{-2}	2.83	0.999	11.509
0.251–0.178	3.66	0.60×10^{-2}	1.05	2.17×10^{-2}	3.68	0.999	12.522

travel longer distance. In other words, the diffusion path of 2,4-D molecules is longer in larger particles than in smaller particles, and hence they take more time to reach equilibrium. This is due to higher intraparticle diffusion resistance and lower internal diffusion coefficient for higher particle size of the adsorbent[10].

Kinetics of adsorption

The pseudo first-order (PFO) and pseudo second-order (PSO) kinetic models were applied to experimental data. Equations (4) and (5) represent the linear form of PFO and PSO kinetic models respectively[29]

$$\ln(Q_e - Q_t) = \ln Q_e - k_1 t, \tag{4}$$

$$\frac{t}{Q_t} = \frac{1}{k_2 Q_e^2} + \frac{t}{Q_e}, \tag{5}$$

where k_1 (min^{-1}) and k_2 (g mg^{-1} min^{-1}) are kinetic rate constants, while Q_e (mg/g) and Q_t (mg/g) are the adsorbent capacities at equilibrium and at any time respectively. The half adsorption time (min), $t_{1/2}$, is the time needed for the adsorbent to take up half as much adsorbate as at equilibrium. $t_{1/2}$, as given below, is often considered to measure adsorption rate

$$t_{1/2} = \frac{1}{k_2 Q_e}. \tag{6}$$

The experimental equilibrium capacities are in agreement with those predicted by the PSO kinetic model (Table 5). The coefficients of determination (R^2) are close to unity for PSO. Thus the PSO kinetic model fits better for the given system. Therefore, it can be deduced that the adsorption of 2,4-D on different particle sizes of RHA is predominantly controlled by the number of available adsorption sites rather than the concentration of 2,4-D (ref. 23). As indicated in Table 5 for PSO, k_2 is inversely proportional and Q_e, is directly proportional to particle size and thereby characteristics (pore geometry and silica to carbon ratio). The half adsorption time is increases with increase in particle size, which indicates no significant resistance to intraparticle pore diffusion for smaller particles compared to larger particles[12].

Conclusion

The physico-chemical characteristics of BMA play a vital role in determining capacity and kinetics of adsorption. Chemical composition and surface functional groups of BMA are qualitatively similar. Carbon content controls the adsorption capacity, while silica controls the kinetics. BMA is mesoporous in nature. Adsorption capacity and equilibrium time for larger particles are higher. Larger particles have deeper pores with smaller opening, whereas small particles have shallow pores with wider opening. This causes faster diffusion leading to higher kinetic constant in smaller particles. Thus BMA is an effective adsorbent for the removal of anionic species.

1. Ministry of New and Renewable Energy, Government of India (GoI); http://www.mnre.gov.in/schemes/grid-connected/biomass-powercogen (accessed on 10 July 2014).
2. Khan, R., Jabbar, A., Ahmad, I., Khan, W., Khan, A. N. and Mirza, J., Reduction in environmental problems using rice-husk ash in concrete. *Constr. Build. Mater.*, 2012, **30**, 360–365.
3. Akram, T., Memon, S. A. and Obaid, H., Production of low cost self compacting concrete using bagasse ash. *Constr. Build. Mater.*, 2009, **2**, 703–712.
4. Directorate of Economics and Statistics, Ministry of Agriculture, GoI; http://eands.dacnet.nic.in/latest_2006.htm (accessed on 10 July 2014).
5. Bhatnagar, A. and Sillanpaa, M., Utilization of agro-industrial and municipal waste materials as potential adsorbents for water treatment – a review. *Chem. Eng. J.*, 2010, **157**, 277–296.
6. Madurwar, M. V., Ralegaonkar, R. V. and Mandavgane, S. A., Application of agro-waste for sustainable construction materials: a review. *Constr. Build. Mater.*, 2013, **38**, 872–878.
7. Wan Ngah, W. S. and Hanafiah, M. A. K. M., Removal of heavy metal ions from wastewater by chemically modified plant wastes as adsorbents: a review. *Bioresour. Technol.*, 2008, **99**, 3935–3948.
8. Ahmaruzzaman, M. and Gupta, V. K., Rice husk and its ash as low-cost adsorbents in water and wastewater treatment. *Ind. Eng. Chem. Res.*, 2011, **50**, 13589–13613.

9. Aksu, Z. Application of biosorption for the removal of organic pollutants: a review. *Process Biochem.*, 2005, **40**, 997–1026.
10. Sag, Y. and Aktay, Y., Mass transfer and equilibrium studies for the sorption of chromium onto chitin. *Process Biochem.*, 2000, **36**, 157–173.
11. Gupta, V. K., Mohan, D., Suhas and Singh, K. P., Removal of 2-aminophenol using novel adsorbents. *Ind. Eng. Chem. Res.*, 2006, **45**, 1113–1122.
12. Gupta, V. K., Mittal, A., Krishnan, L. and Mittal, J., Adsorption treatment and recovery of hazardous dye, brilliant blue FCF, over bottom ash and de-oiled soya. *J. Colloid Interface Sci.*, 2006, **293**, 16–26.
13. Tsai, W. T., Lai, C. W. and Hsien, K. J., Effect of particle size of activated clay on the adsorption of paraquat from aqueous solution. *J. Colloid Interface Sci.*, 2003, **263**, 29–34.
14. Umamaheswaran, K. and Batra, V. S., Physico-chemical characterisation of Indian biomass ashes. *Fuel*, 2008, **87**, 628–638.
15. Pavia, D. L., Lampman, G. M., Kriz, G. S. and Vyvyan, J. R., *Introduction to Spectroscopy*, Cengage Learning, USA, 2008, 4th edn.
16. Mall, I. D., Srivastava, V. C., Agarwal, N. K. and Mishra, I. M., Adsorptive removal of malachite green dye from aqueous solution by bagasse fly ash and activated carbon-kinetic study and equilibrium isotherm analyses. *Colloids Surf. A*, 2005, **264**, 17–28.
17. Tailor, R., Shah, B. and Shash, A., Sorptive removal of phenol by zeolitic bagasse fly ash: equilibrium, kinetics and column studies. *J. Chem. Eng. Data*, 2012, **57**, 1437–1448.
18. Totlani, K., Mehta, R. and Mandavgane, S. A., Comparative study of adsorption of Ni (II) on RHA and carbon embedded silica obtained from RHA. *Chem. Eng. J.*, 2012, **181–182**, 376–386.
19. Srivastava, V. C., Mall, I. D. and Mishra, I. M., Characterization of mesoporous rice husk ash (RHA) and adsorption kinetics of metal ions from aqueous solution onto RHA. *J. Hazard. Mater. B*, 2006, **134**, 257–267.
20. Infrared analysis of organosilicon compounds: spectra–structure correlations; http://www.gelest.com/goods/pdf/Library/11Infra.pdf (accessed on 16 August 2014).
21. Salman, J. M., Njoku, V. O. and Hameed, B. H., Adsorption of pesticides from aqueous solution onto banana stalk activated carbon. *Chem. Eng. J.*, 2011, **174**, 41–48.
22. Hameed, B. H., Salman, J. M. and Ahmad, A. L., Adsorption isotherm and kinetic modeling of 2,4-D pesticide on activated carbon derived from date stones, *J. Hazard. Mater.*, 2009, **163**, 121–126.
23. Njokua, V. O. and Hameed, B. H., Preparation and characterization of activated carbon from corncob by chemical activation with H_3PO_4 for 2,4-dichlorophenoxyacetic acid adsorption. *Chem. Eng. J.*, 2011, **173**, 391–399.
24. Tang, L. *et al.*, Rapid adsorption of 2,4-dichlorophenoxyacetic acid by iron oxide nanoparticles-doped carboxylic ordered mesoporous carbon. *J. Colloid Interface Sci.*, 2015, **445**, 1–8.
25. Zhang, F., Song, Y., Song, S., Zhang, R. and Hou, W., Synthesis of magnetite–graphene oxide-layered double hydroxide composites and applications for the removal of Pb(II) and 2,4-dichlorophenoxyacetic acid from aqueous solutions. *Appl. Mater. Interfaces*, 2015, **7**, 7251–7263.
26. Mahramanlioğlu, M., Kizilcikli, I., Biçer, Đ. O. and Tunçay, M., Removal of 2,4-D from aqueous solution by the adsorbents from spent bleaching earth. *J. Environ. Sci. Health B.*, 2000, **35**, 187–200.
27. Srivastava, V. C., Mall, I. D. and Mishra, I. M., Equilibrium modelling of single and binary adsorption of cadmium and nickel onto bagasse fly ash. *Chem. Eng. J.*, 2006, **117**, 79–91.
28. Lataye, D. H., Mishra, I. M. and Mall, I. D., Adsorption of 2-picoline onto bagasse fly ash from aqueous solution. *Chem. Eng. J.*, 2008, **138**, 35–46.
29. Dogan, M., Alkan, M., Turkyilmaz, A. and Ozdemir, Y., Kinetics and mechanism of removal of methylene blue by adsorption onto perlite. *J. Hazard. Mater. B*, 2004, **109**, 141–148.

ACKNOWLEDGEMENTS. We thank the Science and Engineering Research Board, India for providing research grant (SB/S3/CE/077/2013) to undertake the work. We also thank IBM, Nagpur and CSMCRI, Bhavnagar for providing sophisticated characterization facilities and Dr Sayaji Mehtre (BARC, Mumbai) for assistance in characterization.

Received 26 February 2015; revised accepted 28 September 2015

doi: 10.18520/cs/v110/i2/180-186